Near-offset interpolation in wavefront synthesis imaging

Jun Ji [1]

ABSTRACT

Missing near-offset traces play an important role in wavefront synthesis imaging. The effect of missing near-offset traces appears as a weak or broken image from place to place according to the reflector geometry and the angle of planewave synthesized. This paper describes an interpolation scheme I have developed to fill in the missing near-offset traces. The missing near-offset traces can be interpolated by using the fact that all reflection events are hyperbolic in a common-midpoint (CMP) gather. Therefore, I find an optimum velocity spectrum of a CMP gather and fill in missing traces by hyperbolic modeling with the optimum velocity spectrum.

INTRODUCTION

The ideal acquisition geometry for wavefront synthesis is a fixed split spread with infinite aperture. In practice, however, a moving one-side spread with finite receiver length is the typical acquisition geometry in marine surveys. The moving one-side spread acquisition leaves missing traces at near and far offsets. These missing traces cause a weak or broken image from place to place according to the reflector geometry and the angle of planewave synthesized.

If we are only interested in structural imaging, weak or broken images are not a big problem. Such image defections will disappear after the stacking of several images generated by different planewave synthesis. If we are interested in angle-dependent reflectivity, however, each image from a different planewave needs to be analyzed separately. Therefore, the missing traces should be interpolated to get a complete image without defects in it.

[1] **email:** jun@sep.stanford.edu

In this paper, I introduce an interpolation scheme for missing traces in near and far offset. First, I review the forward model of a shot experiment and wave stack that allows the wavefront synthesis. Then the detailed algorithm of the interpolation scheme is presented, along with some examples of synthetic and Marmousi datasets.

WAVEFRONT SYNTHESIS USING WAVE STACKS

After preprocessing for multiple reflections, the monochromatic 2-D forward model for a seismic shot record can be written as follows (Berkhout, 1985):

$$\mathbf{g}_j(z_0) = F(z_0, z_0)\mathbf{s}_j(z_0) \tag{1}$$

with

$$F = \sum_{n=1}^{N} W(z_0, z_n)R(z_n)W(z_n, z_0). \tag{2}$$

In equation (**??**) source vector $\mathbf{s}_j(z_0)$ and measurement vector $\mathbf{g}_j(z_0)$ refer to one seismic experiment at the surface $z = z_0$ with source location at $x = x_j$. In equation (**??**) propagation operators $W(z_n, z_0)$ and $W(z_0, z_n)$ quantify the full propagation effects (down and up, respectively) between depth levels z_0 and z_n, and reflection matrix $R(z_n)$ defines the elastic angle-dependent reflection properties caused by inhomogeneities at depth level z_n. All matrices and vectors refer to one temporal Fourier component. Equations (**??**) and (**??**) are valid for single-component as well as multi-component measurement of 2-D as well as 3-D data (Berkhout, 1992). This report, however, is restricted to the 2-D acoustic case.

A *wave stack* is any stack over a common shot or geophone gather in which the moveout is independent of time (Schultz and Claerbout, 1978). It synthesizes a particular wavefront of raw data because Huygens's principle permits the synthesis of arbitrarily shaped downward propagating wavefronts from the superposition of many spherical wavefronts. Unlike the common midpoint stack, wave stacks retain the important property of being the sampling of a real possible wave fields and, as such, permit the treatment of formerly difficult or impossible problems with the use of the wave equation.

The forward operator in equation (**??**) is independent of time, so any linear combination of the recorded trace can be expressed by a combination of source functions as follows :

$$\sum_{j=1}^{M} \gamma_j \mathbf{g}_j(z_0) = F(z_0, z_0) \sum_{j=1}^{M} \gamma_j \mathbf{s}_j(z_0), \tag{3}$$

where M is the number of source functions used for wave stacking, and γ_j is any complex value. The γ_j controls the wavefront by scaling and phase shifting. Therefore, we can control the wavefront by adjusting γ_j appropriately.

EFFECTS OF APERTURE

The ideal acquisition pattern for plane-wave synthesis is a fixed split spread with wide aperture (Figure ??). With this acquisition, every receiver will record reflected wavefields caused by every source wavefield. In practice, however, a moving one-side spread (Figure ??) is the typical acquisition pattern in marine surveys.

The forward model in equation (??) implicitly assumes an infinite aperture experiment. In order to formulate the forward model correctly, we need to incorporate the aperture effect, as follows:

$$\mathbf{g}_j(z_0) = A_j F(z_0, z_0)\mathbf{s}_j(z_0), \tag{4}$$

where A_j is a diagonal matrix with 1 at the receiver position and 0 elsewhere. Since the aperture operator, A_j, changes from source to source in a moving one-side spread acquisition, the wave-stack equation (??) is no longer valid. In order to overcome this problem, we need to fill the missing traces before wave stacking.

In the case of the one-sided spread acquisition, we can expand the acquisition area using the principle of reciprocity, which states that if we exchanged the source and receiver positions, we would record the same seismic trace at the source position. The acquisition pattern expanded using the principle of reciprocity is depicted in Figure ??.

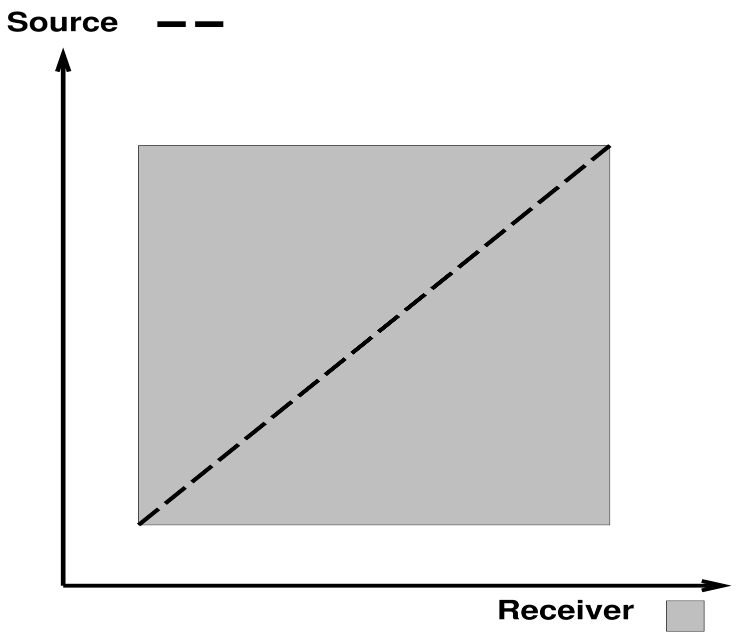

Figure 1: A fixed split-spread acquisition that is ideal for wavefront synthesis imaging. $\boxed{\text{ideal-acq}}$ [NR]

However, Figure ?? shows that we still have some missing regions in near and far offset after the acquisition expansion using the principle of reciprocity. The missing part of the far-offset limits the angle coverage of the reflectivity information. Since the

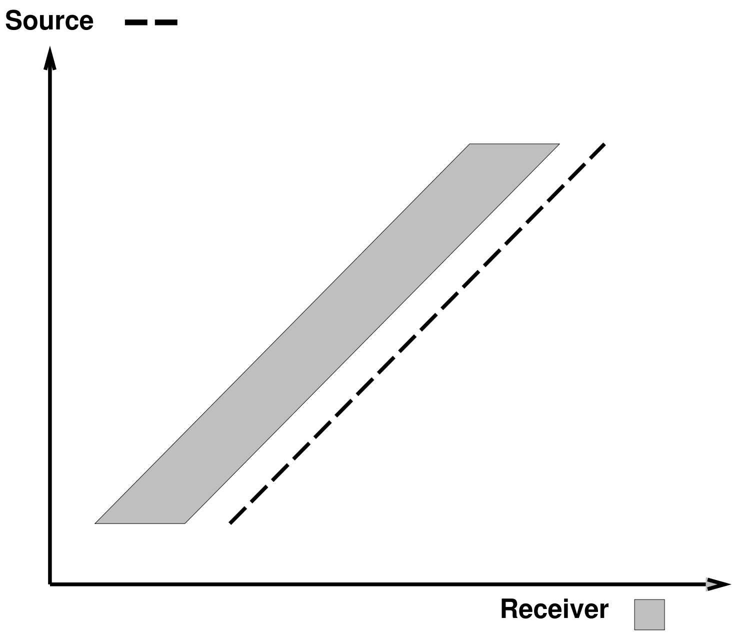

Figure 2: A one-side spread acquisition, which is the typical acquisition pattern in marine surveys. real-acq [NR]

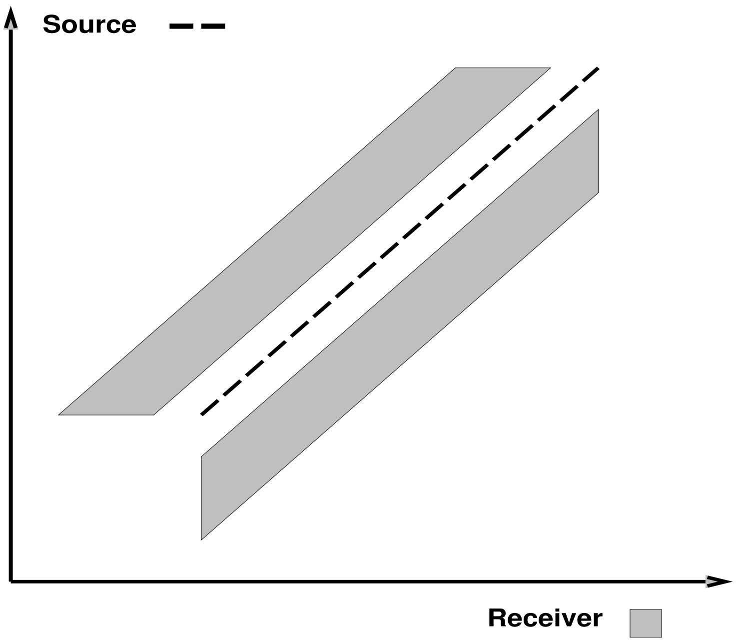

Figure 3: The expanded acquisition pattern from the one-side spread using reciprocity. There are missing regions in the near and far offset. recp-acq [NR]

maximum incidence angle of the source wavefield generally decreases as the depth of the reflector increases (Figure **??**), we can avoid the effects of cable length by limiting the incidence angle ranges of synthesized wavefront differently at every depth level.

The effects of the missing part of the near-offset are not as easy to avoid as those of the missing part of the far offset because they differ in terms of missing reflection angle ranges from depth to depth and are located around the normal incidence angle to reflectors (Figure **??**). In order to obtain a good image for every constant angle illumination, we need to interpolate the missing near-offset traces.

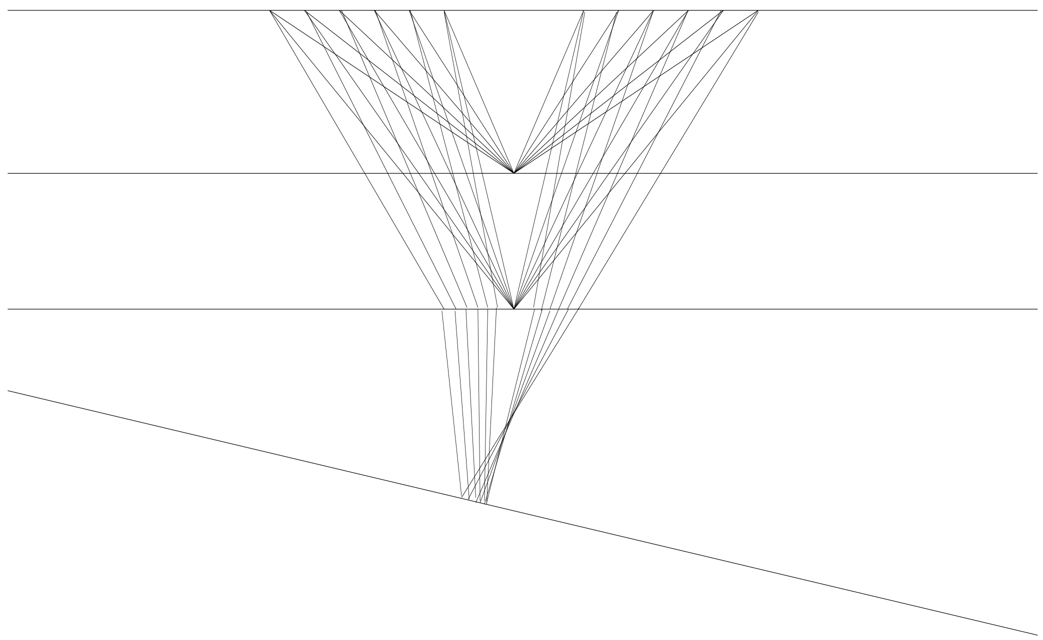

Figure 4: Ray paths for a CMP gather. The maximum incidence angle at each reflector generally decreases as the depth of the reflector increases. Missing near- offset affects the determination of the normal incidence reflectivity of reflectors. ang-cov [NR]

INTERPOLATION OF MISSING NEAR AND FAR OFFSETS

What we want, to interpolate the missing traces, is some events that are extended from the recorded events. Since all reflection events are hyperbolic in CMP gathers, CMP gathers provide evidence of missing traces. Therefore, if we find the velocity spectrum that most closely produces the known data in a CMP gather, we can predict the missing data by hyperbolic modeling from the velocity spectrum.

Thus, the interpolation of missing near-offset traces can be achieved in two steps. The first step is to find the best velocity spectrum from the known traces in each CMP gather. The search for the optimum velocity spectrum in the CMP gather can be formulated, in the least-squares sense, as

$$0 \simeq (\mathbf{d}_k - H\mathbf{m})^2, \tag{5}$$

where $\mathbf{d}_k$ represents the known data in a CMP gather, $\mathbf{m}$ is the velocity spectrum, and H is the hyperbolic modeling operator of the given velocity spectrum.

The second step is to model the missing traces from the optimum velocity spectrum, as follows:

$$\mathbf{d}_m = H\mathbf{m}. \tag{6}$$

I have tested a simple synthetic CMP gather to verify this approach. First, I put three spikes in a velocity spectrum and modeled a CMP gather by spreading the spectrum energy along the hyperbola, and then convolved the CMP gather with a Ricker wavelet (Figure **??**). In order to model possible amplitude-versus-offset (AVO) effect, I scaled each hyperbolic event differently with respect to offset. Figure **??** shows the interpolated CMP gather using the least-squares conjugate gradient algorithm. Because of the smoothness of the optimum velocity spectrum found by the least-squares method, the interpolated traces are close to the other traces in the near-offset but not in the far offset.

In order to make the interpolated traces close to the other known traces, we need a more spiky optimum velocity spectrum. since the spikiness in the velocity spectrum depend on the aperture of the CMP gather and the larger a aperture is, the spikier a velocity spectrum is. To make the optimum velocity spectrum spikier, I used an adaptive weighting factor in the conjugate gradient. The velocity spectrum of the preceding step in each iteration is a good candidate for this problem, because, after the first iteration, the velocity spectrum has larger values where we want the spiky spectrum than elsewhere. Thus, I solve the following adaptive weight least-squares problem

$$0 \simeq (\mathbf{d}_k - HW_i\mathbf{m}_i)^2 \tag{7}$$

with

$$W_i = \sqrt{|m_{i-1}|}.$$

In equation (**??**), the subscript i represents the step of the iteration in the conjugate gradient. Figure **??** shows the interpolated CMP gather obtained by the adaptive weight least-squares method. Now we have an interpolated trace in the near and far offset that is closer to the known traces.

EXAMPLES FROM THE MARMOUSI DATASET

In order to see the effects of missing traces in a complex model, I tested the method on the well-known Marmousi dataset. Figure **??** shows a CMP gather at 7500 meters along the surface location. The right half of the CMP gather is appended using the reciprocity principle. The interpolated gather appears in Figure **??**, which shows that the interpolated traces are very close to the known traces. Figures **??** and **??** show a common-shot gather before and after interpolation, respectively; the interpolated traces follow the pattern of the other known reflection events very closely.

To examine the effects of missing traces in wavefront synthesis imaging, I performed the imaging of the Marmousi data with both missing and interpolated near-

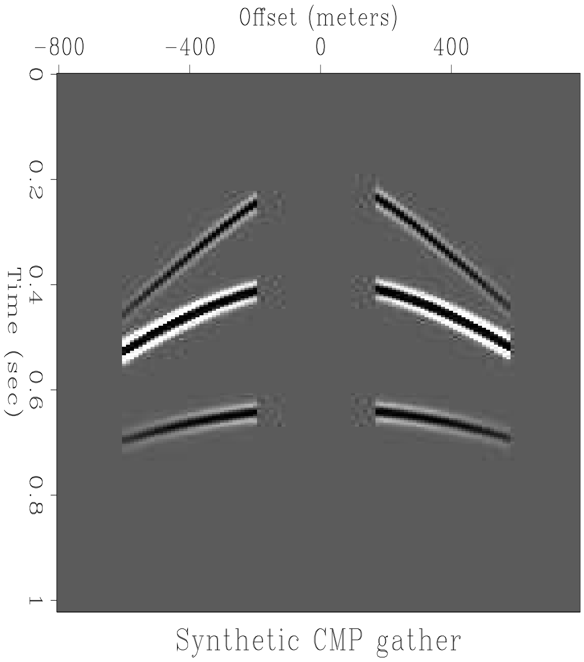

Figure 5: Synthetic CMP gather with three reflectors with missing near and far offset traces. Notice that each hyperbolic event have different AVO efffect. $\boxed{\text{syn-cmp}}$ [R]

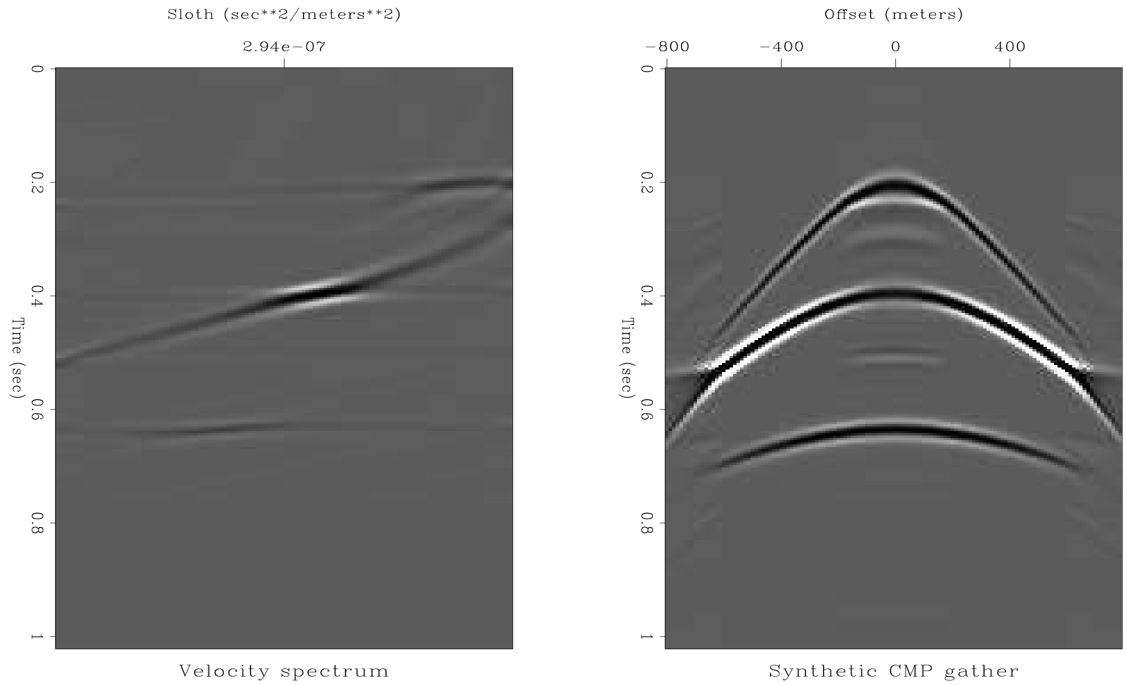

Figure 6: The optimum velocity spectrum (Left) and the interpolated synthetic CMP gather (Right) obtained without weighting in the conjugate gradient iteration step. $\boxed{\text{syn-intcmp}}$ [R]

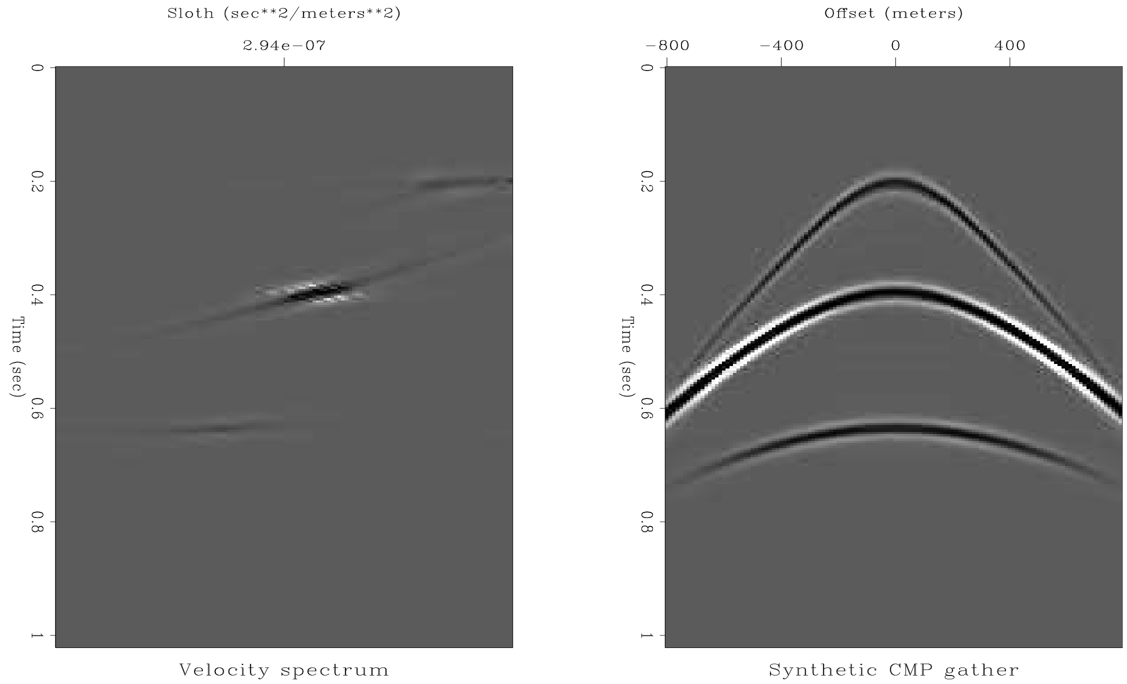

Figure 7: The optimum velocity spectrum (Left) and the interpolated synthetic CMP gather (Right) obtained with weighting in the conjugate gradient iteration step. syn-intcmpww [R]

offset traces. Figures **??** and **??** show the images of a zero-degree planewave with and without missing near-offset traces, respectively. The major difference can be found around the flat reflectors (depth=1500m, surface=7500m). Since the planewave used in these examples travels vertically, most of the reflected energy from the flat reflectors would be in the near-offset. Therefore, the missing near-offset traces mostly affect the image of the flat reflectors.

Figures **??** and **??** show the images of a 10-degree planewave with and without missing near-offset traces, respectively. Again, the major difference appears around the reflector, which is close to 10 degrees (depth=1500m, surface=7500m). This tells us that the missing near-offset traces would affect the image quality of the reflectors whose dips are close to the dip of the synthesized planewave.

CONCLUSIONS

Missing near-offset traces play an important role in wavefront synthesis imaging. The effect of missing near-offset appears as a weak or broken image from place to place according to the reflector geometry and the angle of the planewave synthesized. I have developed an interpolation scheme to fill in the missing near-traces. After finding an optimum velocity spectrum of a common-midpoint (CMP) gather, the missing traces are filled in by hyperbolic modeling with the optimum velocity spectrum. In testing the method with the Marmousi dataset, the weak or broken images caused by missing traces were successfully recovered by the interpolation algorithm.

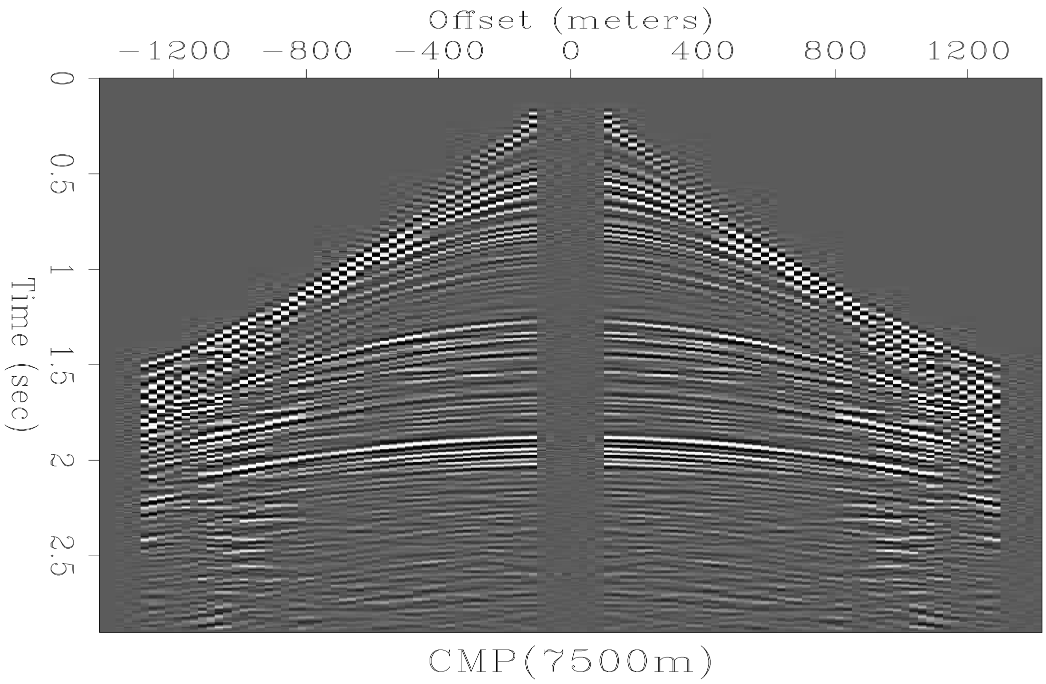

Figure 8: CMP gather at 7500m in the Marmousi dataset. cmp-463 [R]

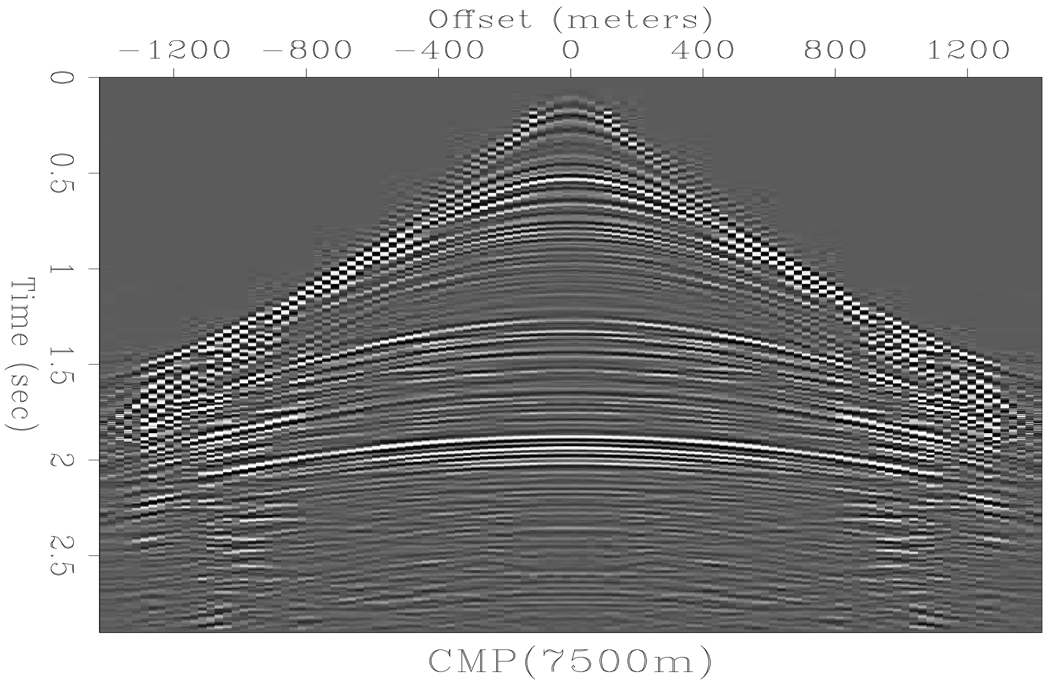

Figure 9: Interpolated CMP gather at 7500m in the Marmousi dataset. intcmp-463 [R]

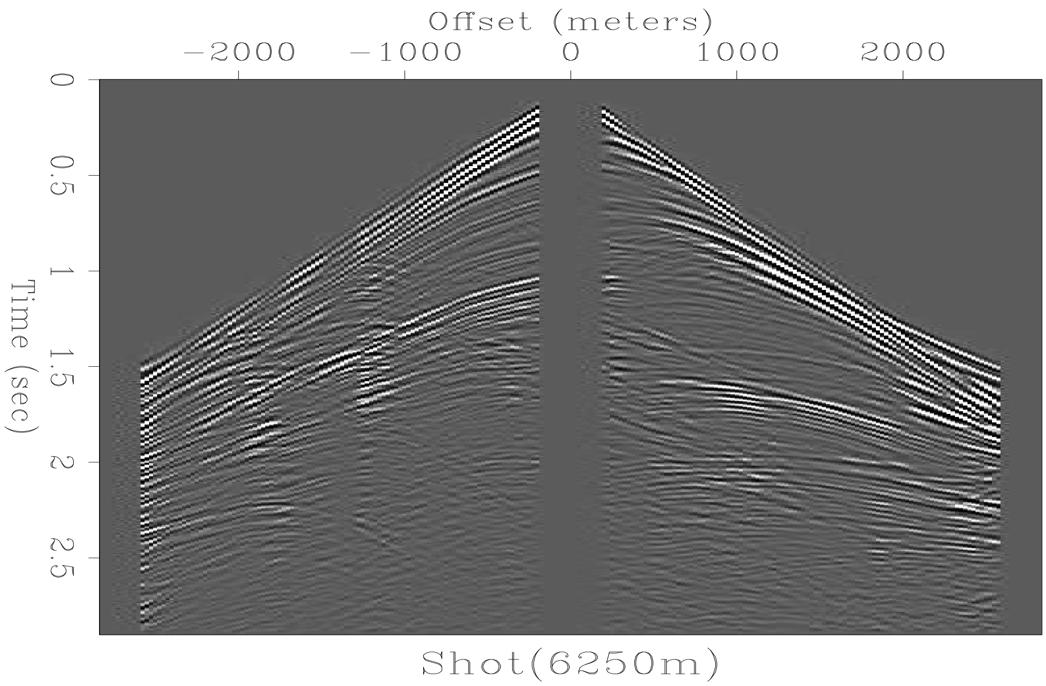

Figure 10: Shot gather at 6250m in the Marmousi dataset. shot-131 [NR]

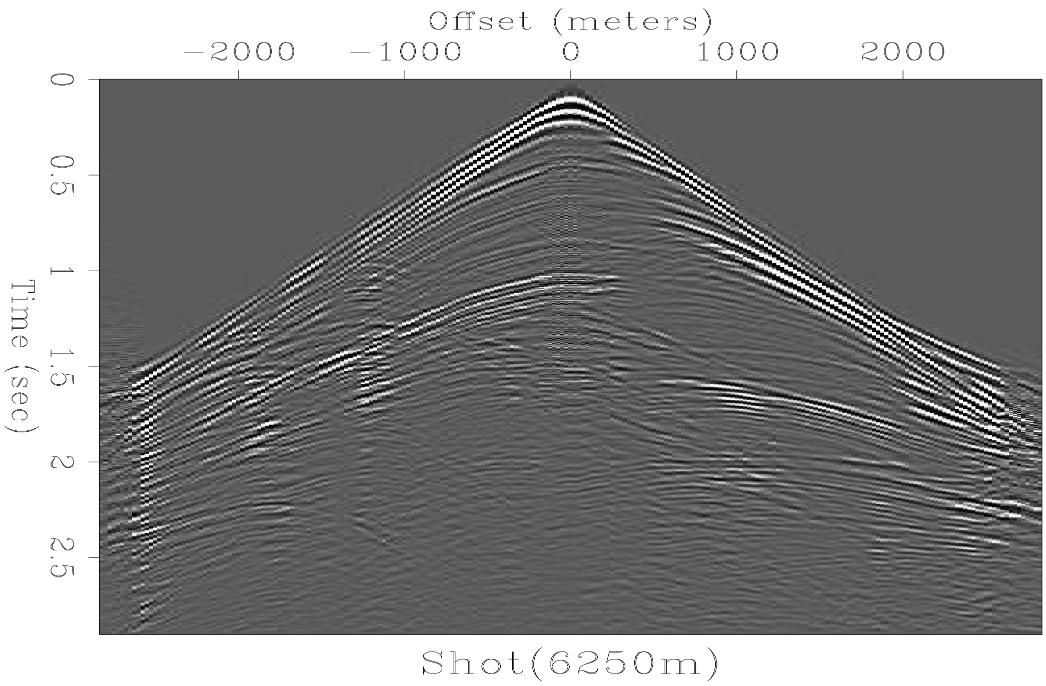

Figure 11: Interpolated Shot gather at 6250m in the Marmousi dataset. intshot-131 [NR]

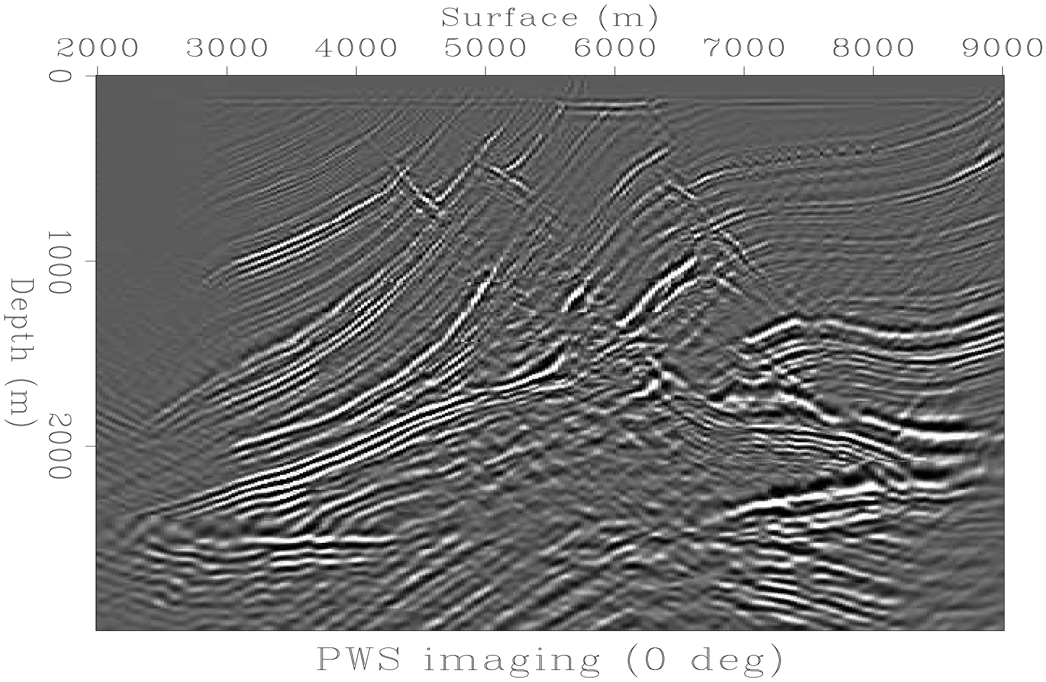

Figure 12: Marmousi image without near-offset traces, obtained by synthesizing a planewave traveling vertically. pws-mar-0 [CR]

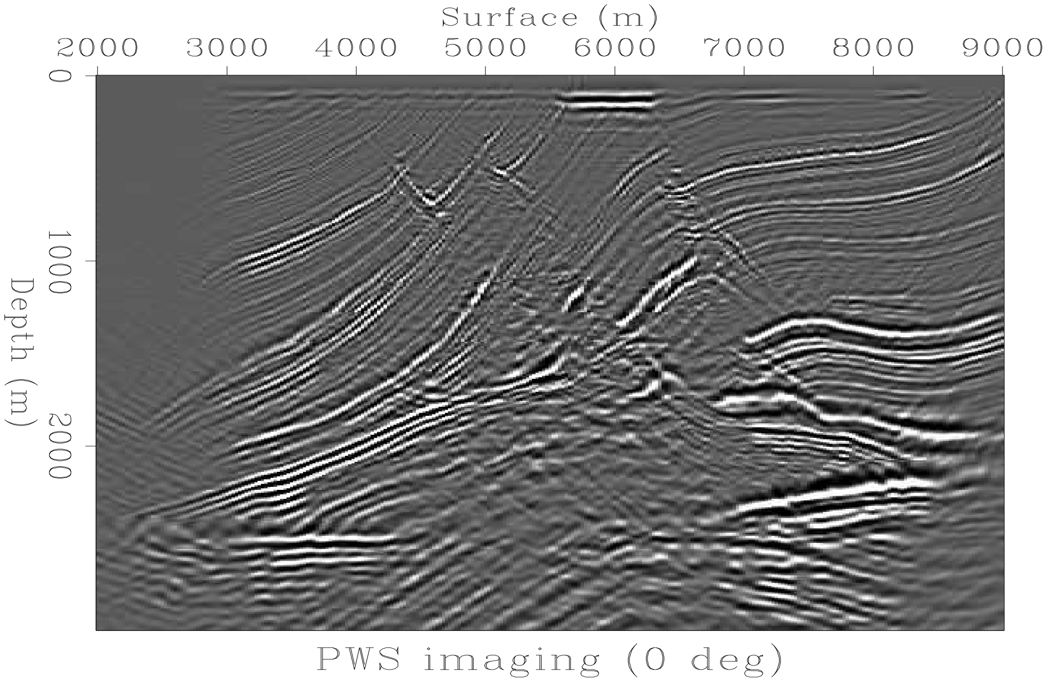

Figure 13: Marmousi image with interpolated near-offset traces, obtained by synthesizing a planewave traveling vertically. pws-marint-0 [CR]

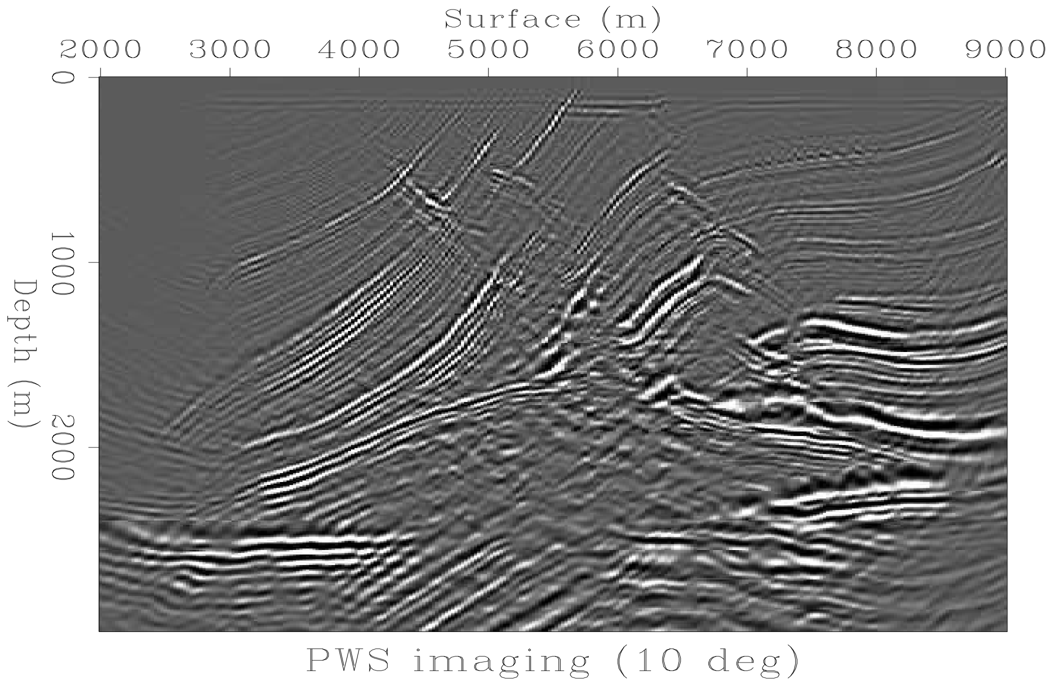

Figure 14: Marmousi image without near-offset traces, obtained by synthesizing a planewave traveling 10 degrees to the vertical. pws-mar-10 [CR]

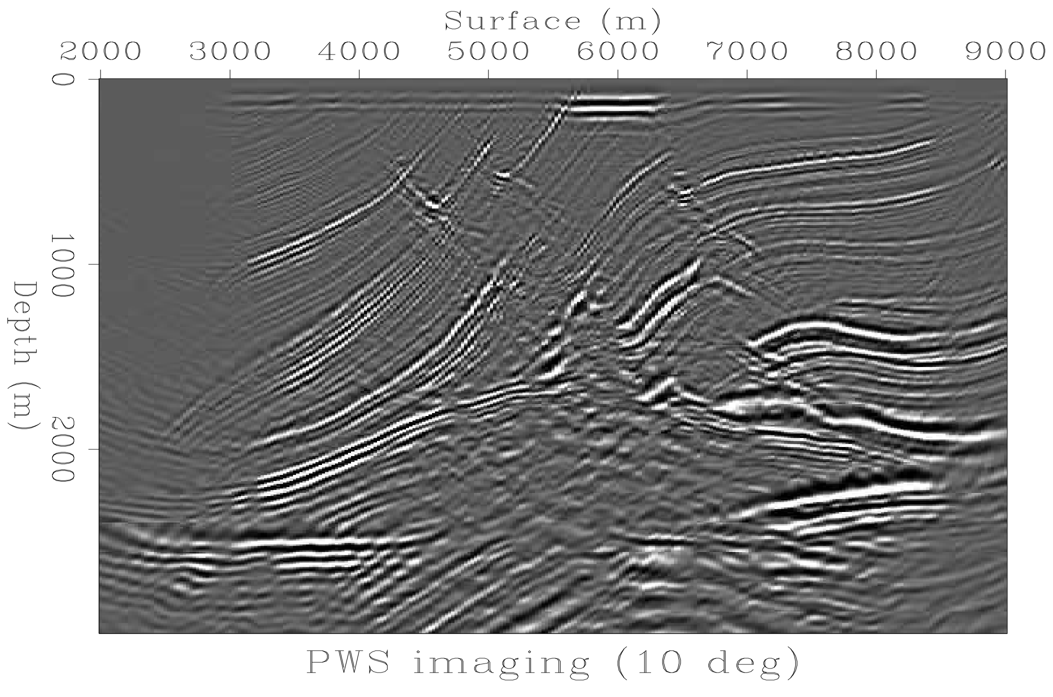

Figure 15: Marmousi image with interpolated near-offset traces, obtained by synthesizing a planewave traveling 10 degrees to the vertical. pws-marint-10 [CR]

REFERENCES

Berkhout, A. J., 1985, Seismic migration: Imaging of acoustic energy by wave field extrapolation. A. Theoretical aspects: Elsevier Science Publ. Co., Inc.

Claerbout, J. F., 1985, Imaging the Earth's Interior: Blackwell Scientific Publications.

Ji, J., 1993, Controlled illumination by wavefront synthesis: SEP–**79**, 129–144.

Rietveld, W. E. A., Berkhout, A. J., and Wapenaar, C. P. A., 1992, Optimum seismic illumination of hydrocarbon reservoirs: Geophysics, **57**, 1334–1345.

Rietveld, W. E. A. and Berkhout, A. J., 1992, Depth migration combined with controlled illumination: 62th Ann. Internat. Mtg., Soc. Expl. Geophys., Expanded Abstracts, 931–934.

Schultz, P. S. and Claerbout, J. F., 1978, Velocity estimation and downward continuation by wavefront synthesis: Geophysics, **43**, 691–714.